Neuronal Dysfunction and Disconnection of Cortical Hubs in Non-Demented Subjects with Elevated Amyloid Burden

doi:10.1093/brain/awr066 Brain 2011: 134; 1635–1646 | 1635

BRAIN
A JOURNAL OF NEUROLOGY

Neuronal dysfunction and disconnection of cortical hubs in non-demented subjects with elevated amyloid burden

Alexander Drzezga,[1,2] J. Alex Becker,[1] Koene R. A. Van Dijk,[1,2,4] Aishwarya Sreenivasan,[2,5] Tanveer Talukdar,[1,2] Caroline Sullivan,[2,3] Aaron P. Schultz,[2,3] Jorge Sepulcre,[1,2,4] Deepti Putcha,[2,3] Doug Greve,[2] Keith A. Johnson[1,3,5] and Reisa A. Sperling[2,3,5]

1 Department of Radiology, Massachusetts General Hospital and Harvard University Medical School, Boston, MA 02114, USA
2 Athinoula A. Martinos Centre for Biomedical Imaging, Suite 2301 Charlestown, MA 02129, USA
3 Centre for Alzheimer Research and Treatment, Department of Neurology, Harvard University Medical School, Brigham and Women's Hospital, Boston, MA 02115, USA
4 Department of Psychology and Centre for Brain Science, Harvard University, Northwest Building, Cambridge, MA 02138, USA
5 Department of Neurology, Massachusetts General Hospital, Harvard University Medical School, Boston, MA 02114, USA

Correspondence to: Alexander Drzezga, MD,
Department of Nuclear Medicine,
Klinikum rechts der Isar,
Technische Universität München,
Ismaningerstr. 22,
81675 Munich,
Germany
E-mail: a.drzezga@lrz.tum.de

Disruption of functional connectivity between brain regions may represent an early functional consequence of β-amyloid pathology prior to clinical Alzheimer's disease. We aimed to investigate if non-demented older individuals with increased amyloid burden demonstrate disruptions of functional whole-brain connectivity in cortical hubs (brain regions typically highly connected to multiple other brain areas) and if these disruptions are associated with neuronal dysfunction as measured with fluorodeoxyglucose-positron emission tomography. In healthy subjects without cognitive symptoms and patients with mild cognitive impairment, we used positron emission tomography to assess amyloid burden and cerebral glucose metabolism, structural magnetic resonance imaging to quantify atrophy and novel resting state functional magnetic resonance imaging processing methods to calculate whole-brain connectivity. Significant disruptions of whole-brain connectivity were found in amyloid-positive patients with mild cognitive impairment in typical cortical hubs (posterior cingulate cortex/precuneus), strongly overlapping with regional hypometabolism. Subtle connectivity disruptions and hypometabolism were already present in amyloid-positive asymptomatic subjects. Voxel-based morphometry measures indicate that these findings were not solely a consequence of regional atrophy. Whole-brain connectivity values and metabolism showed a positive correlation with each other and a negative correlation with amyloid burden. These results indicate that disruption of functional connectivity and hypometabolism may represent early functional consequences of emerging molecular Alzheimer's disease pathology, evolving prior to clinical onset of dementia. The spatial overlap between hypometabolism and disruption of connectivity in cortical hubs points to a particular susceptibility of these regions to early Alzheimer's-type neurodegeneration and may reflect a link between synaptic dysfunction and functional disconnection.

Received October 14, 2010. Revised January 24, 2011. Accepted February 16, 2011. Advance Access publication April 13, 2011

Keywords: amyloid; cortical hubs; functional connectivity; metabolism; mild cognitive impairment; positron emission tomography; magnetic resonance imaging

Abbreviations: FLR-VOI = large cortical volume of interest consisting of frontal, lateral parietal and lateral temporal and retrosplenial cortices; PiB = Pittsburgh compound B

Introduction

The aggregation of β-amyloid peptides has been hypothesized to be causally involved in the genesis of Alzheimer's disease (Braak *et al*., 1999). It has been suggested that neurotoxic amyloid aggregates may lead to synaptic dysfunction and eventually synaptic loss (Selkoe, 2008). Disruption of functional connectivity between brain regions may represent an early deleterious consequence of these synaptic pathologies, potentially occurring prior to neuronal death and atrophy (Greicius *et al*., 2004; Rombouts *et al*., 2005; Hedden *et al*., 2009; Sheline *et al*., 2010).

Multimodal imaging offers a unique opportunity to explore the interrelation and overlap between molecular key pathologies and their functional consequences *in vivo*, even in very early stages of Alzheimer's disease. Characteristic findings have been reported with different imaging techniques in dementia of the Alzheimer's type as well as in predementia stages of disease, such as in mild cognitive impairment and even in healthy at-risk people: increased β-amyloid burden can be measured by ^{11}C-Pittsburgh compound B (PiB)-PET, regional atrophy by structural MRI and reduced neuronal activity is reflected in cerebral hypometabolism as measurable by ^{18}F-fluorodeoxyglucose-PET (Silverman *et al*., 2001; Chetelat *et al*., 2003; Minoshima, 2003; Kantarci and Jack, 2004; Mosconi *et al*., 2004; Dickerson *et al*., 2005; Drzezga *et al*., 2005; Mintun *et al*., 2006; Pike *et al*., 2007; Drzezga, 2008; Okello *et al*., 2009). Recent advances in imaging now allow the assessment of functional connectivity. By measuring the correlation of spontaneous low-frequency activity with resting-state blood oxygen level-dependent functional MRI techniques, synchronously active regions in the brain can be identified, indicating functional interaction of the involved regions (Biswal *et al*., 1995). This technique does not require a cognitive task or active participation by the subject, which may decrease variability due to differences in compliance or performance. Synchronously active brain regions identified by this technique are commonly referred to as 'resting-state networks'. The most prominent example of such a network is the so-called 'default mode network' (Gusnard and Raichle, 2001; Raichle *et al*., 2001). The default mode network includes the posterior cingulate cortex and medial prefrontal, hippocampal and inferior parietal cortical regions, and has been associated with the processing of internally focused cognitive tasks (Buckner *et al*., 2008). Interestingly, a striking topographical resemblance of the default mode network has been described with pathological findings in Alzheimer's disease, i.e. regional hypometabolism, amyloid deposition and regional atrophy (Buckner *et al*., 2005, 2009). Reductions of functional connectivity within the default mode network have been demonstrated in Alzheimer's disease and mild cognitive impairment, particularly in posterior cingulate cortex/precuneus regions (Greicius *et al*., 2004; Rombouts *et al*., 2005; Sorg *et al*., 2007; Fleisher *et al*., 2009). The striking anatomic overlap in the pattern of alterations in Alzheimer's disease across these imaging modalities may indicate an interrelation between different pathomechanisms. Recent studies have shown an association between default mode network disruption and amyloid burden in healthy elderly subjects during task (Sperling *et al*., 2009) and rest conditions (Hedden *et al*., 2009; Sheline *et al*., 2010). However, the association between alterations in synaptic function, functional connectivity and amyloid burden still remains to be elucidated. Typically, resting-state networks have been detected by the identification of brain regions functionally connected to a specific seed region (e.g. the posterior cingulate cortex) or by means of independent component analysis (Calhoun *et al*., 2001; Beckmann *et al*., 2005; Vincent *et al*., 2006; Buckner *et al*., 2008). These strategies allow the identification of specific separate networks but they do not provide independent information with regard to the regional degree of connectivity in any given region in the brain. This fact considerably limits the comparability of functional connectivity findings with results from other imaging modalities such as fluorodeoxyglucose-PET. This limitation may be overcome by recently introduced 'cortical hub analysis' of resting-state functional MRI data, which allows identification of the number of functionally connected voxels for every single voxel in the brain. In this technique, the time course of the blood oxygen level-dependent signal in a target voxel is extracted and correlated to the time course of every other voxel across the entire brain, yielding a whole-brain connectivity value, based on the number of voxels it is strongly correlated with (Buckner *et al*., 2009; Sepulcre *et al*., 2010). Regions that are functionally connected to many other brain regions are referred to as 'cortical hubs'. It has been speculated that cortical hubs may play an important role in moderating inter-regional neuronal communication (Buckner *et al*., 2009; Tomasi and Volkow, 2010).

Previous work from our group suggested that the anatomic distribution of amyloid burden in patients with Alzheimer's disease overlapped with the cortical hub regions with highest cortical connectivity in young subjects (Buckner *et al*., 2009). We aimed to test the premise that increasing amyloid burden in the brain leads to synaptic dysfunction in cortical hubs, resulting in decreased regional neuronal activity and functional disconnection of these regions. Based on results from previous unimodal imaging studies, we speculated that abnormalities would converge particularly in the posterior cingulate cortex/precuneus region, potentially prior to the clinical onset of dementia. To our knowledge, changes in cortical hub integrity have not yet been documented in Alzheimer's disease, mild cognitive impairment or amyloid-positive healthy controls. We employed a multimodal imaging approach in groups of asymptomatic healthy older adults with and without amyloid pathology and also in amyloid-positive subjects with mild cognitive impairment, in order to investigate the relationship

between amyloid burden, local neuronal function and whole-brain functional connectivity in predementia stages of Alzheimer's disease.

Materials and methods

Subject inclusion

The subjects included in this study were selected from a larger population of 76 subjects who had participated in an ongoing study on cognition and ageing at Brigham and Women's Hospital and Massachusetts General Hospital, including a multimodal imaging protocol consisting of ^{18}F-fluorodeoxyglucose-PET, ^{11}C-PiB-PET, structural MRI and resting state functional MRI, as well as detailed neuropsychological evaluation (for detailed in/exclusion criteria see Supplementary Material). From this population, we aimed to select three groups of subjects: (i) healthy older controls without cortical uptake of ^{11}C-PiB (PiB-negative), i.e. subjects without evidence of pathological cortical amyloid deposition; (ii) PiB-positive healthy control subjects and (iii) PiB-positive subjects with mild cognitive impairment, representing a high-risk population for Alzheimer's disease.

Only amyloid-positive patients with mild cognitive impairment were selected, to avoid inclusion of subjects potentially suffering from disorders other than Alzheimer's disease (Cohen *et al*., 2009). Clinical classification was performed employing established criteria (see Supplementary material) and classification into PiB-positive or PiB-negative was performed on the basis of pre-established thresholds of cortical ^{11}C-PiB distribution, as described below (Johnson *et al*., 2007; Gomperts *et al*., 2008; Hedden *et al*., 2009). For statistical purposes, we tried to select as large as possible groups from the pre-existing population, with the constraint that the three groups would not differ with regard to age, level of education, time intervals between their examinations and that they had successfully undergone all imaging procedures and completed all neuropsychological tests.

All subjects provided written informed consent prior to any experimental procedures in accordance with protocols approved by the Partners Healthcare Inc. Institutional Review Board. The study was approved by and conducted under the auspices of the Partners Human Research Committee at Brigham and Women's Hospital and Massachusetts General Hospital. A subset of data on PiB-positive and PiB-negative healthy controls as well as from eight subjects with mild cognitive impairment in this study have been included in previous publications (Hedden *et al*., 2009; Sperling *et al*., 2009). However, neither the whole-brain connectivity analysis of resting-state functional MRI, nor the fluorodeoxyglucose-PET data in these subjects, nor any cross-modal interaction between these imaging parameters or their association with amyloid load has been published previously.

Image acquisition and analysis

All acquisition, preprocessing and image analysis procedures of structural MRI, functional MRI, ^{18}F-fluorodeoxyglucose-PET and ^{11}C-PiB-PET were conducted using standard procedures as published previously (see below for detailed references).

Magnetic resonance imaging

All MRI-data were acquired on a Siemens Trio 3.0 T MRI-scanner (Siemens Medical Systems) as published previously (Sperling *et al*., 2009). For structural MRI/voxel-based morphometry, high-resolution T_1-weighted structural images were acquired [3D magnetization prepared rapid acquisition gradient echo (MP-RAGE) sequences: repetition time = 2530 ms, echo time = 3.45 ms, inversion time = 1100 ms, flip angle = 7°, field of view = 256 mm, matrix 192 × 256, slice thickness = 1.33 mm, 128 sagittal slices]. Preprocessing of structural MRI data and voxel-based morphometry analysis was carried out using SPM5 software as recently reported (Drzezga *et al*., 2009). T_1-weighted high-resolution structural MRI data were spatially normalized to the MRI Montreal Neurological Institute template in SPM5 and warping parameters were collected for later normalization of PET data (Drzezga *et al*., 2008). Default SPM5 software was used, applying the unified segmentation process (Ashburner and Friston, 2005) and images were segmented into grey and white matter and CSF. Then, the modulated grey matter images were selected for further analysis. Voxel-by-voxel *t*-tests were applied to detect grey matter differences between the different subject groups (Sorg *et al*., 2007). This approach has been previously demonstrated to be suitable for voxel-based morphometry analysis of patients with dementia, even with marked brain atrophy (Jack *et al*., 2008) (see also Supplementary material).

For resting functional MRI, blood oxygen level-dependent functional MRI data were acquired using a T_2*-weighted gradient echo echo-planar imaging (EPI) sequence: repetition time = 2000 ms, echo time = 30 ms, flip angle = 90°, field of view = 200 mm, matrix = 64 × 64. Thirty slices oriented perpendicular to the anterior–posterior commissure line, with 5-mm thick slices and 1-mm gap and 3.125 × 3.125 mm in-plane resolution, were acquired in each of the functional volumes, with 195 whole-brain volumes acquired in the run. Five 'dummy' scans were collected at the beginning of the resting run to allow for T_1 equilibration effects. The resting run lasted 6 min 40 s. During the resting run, subjects were instructed to fixate on a visual white cross-hair, centred on a black background. Functional MRI preprocessing included compensation of systematic, slice-dependent time shifts, motion correction and normalization to the atlas space of the Montreal Neurological Institute (SPM2; Wellcome Department of Cognitive Neurology) resulting in volumetric time series resampled at 2 mm cubic voxels. Temporal filtering retained frequencies below 0.08 Hz, spatial smoothing was performed using a 4-mm full-width half maximum Gaussian blur. Non-specific variance was removed by regression of nuisance variables such as head motion, signal averaged over whole brain, ventricles and white matter (for details see Supplementary Material).

Functional connectivity analysis (cortical hub analysis) was carried out in the current study as previously reported (Buckner *et al*., 2009). The time course of the blood oxygen level-dependent signal in a target voxel was extracted and correlated to the time course of every other voxel across the entire brain (Buckner *et al*., 2009). The number of strongly connected voxels was then assigned to this target voxel as whole-brain connectivity value. This procedure was repeated for every voxel in the brain and a whole-brain connectivity map, showing the degree values of whole-brain connectivity for every voxel in the brain, was produced for every subject, with a high whole-brain connectivity value representing high connectivity to the rest of the brain. These maps formed the basis for further statistical analyses.

Positron emission tomography

All PET scans were acquired on a Siemens/CTI ECAT HR$^+$ PET scanner as described below. Amyloid imaging was performed with *N*-methyl-^{11}C-2-(4-methylaminophenyl)-6-hydroxybenzothiazole (PiB). ^{11}C-PiB was prepared as described by Mathis *et al*. (2002) and PiB-PET scans were acquired at Massachusetts General Hospital, as previously described (Johnson *et al*., 2007; Gomperts *et al*., 2008; Hedden

et al., 2009; Sperling et al., 2009). Following a transmission scan, 10–15 mCi ^{11}C-PiB was injected as a bolus intravenously and followed immediately by a 60-min dynamic PET scan in 3D mode (63 image planes, 15.2 cm axial field of view, 5.6 mm transaxial resolution and 2.4 mm slice interval; 69 frames: 12 × 15 s, 57 × 60 s). PiB-PET data were reconstructed with ordered set expectation maximization, corrected for attenuation and each frame was evaluated to verify adequate count statistics and absence of head motion. Individual ^{11}C-PiB-PET scans were spatially normalized using the warping information derived from individual stereotactic normalization of the structural MRI using SPM 5. The Logan graphical analysis method was used to calculate distribution volume ratios, with the cerebellar cortex as the reference tissue (Price et al., 2005). In analogy to previously published studies (Hedden et al., 2009), a pre-established large cortical volume of interest consisting of frontal, lateral parietal and lateral temporal and retrosplenial cortices (FLR-VOI) was used to evaluate amyloid burden. Distribution volume ratios were calculated, using the cerebellar cortex as the reference tissue and previously published cut-off values were used to divide between PiB-positive ($\geqslant$1.15) and PiB-negative ($<$1.15) subjects (Johnson et al., 2007; Gomperts et al., 2008; Hedden et al., 2009).

For ^{18}F-fluorodeoxyglucose-PET imaging, 5.0 ± 1.0 mCi was intravenously injected while subjects were quietly resting. After a 45-min uptake period fluorodeoxyglucose-PET images were acquired for 30 min in 3D mode, following a transmission scan. Image processing was carried following previously established protocols (Drzezga et al., 2008; Yakushev et al., 2008) including normalization and spatial warping using SPM5 software (Friston et al., 1995). These normalized scans were then used for further statistical analyses.

Statistical analysis

Group comparisons

Voxel-based group comparisons were carried out using voxel-by-voxel two-sample *t*-tests (unpaired) in SPM5, as performed in previous studies (Ashburner and Friston, 2005; Ziolko et al., 2006; Drzezga et al., 2008, 2009; Jack et al., 2008). In prior studies, a strong regional overlap between the typical anatomy of the default mode network in healthy controls and the typical patterns of atrophy and hypometabolism in Alzheimer's disease has been noted (Buckner et al., 2005). Interestingly, a strong anatomic overlap between these patterns and the location of the major cortical hub regions, as identified by whole-brain connectivity analysis in healthy control subjects, has also been demonstrated (Buckner et al., 2009). Consequently, we expected that our findings would also be located within this cerebral network. In detail, this network of expected abnormalities included the following regions: ventral medial prefrontal cortex [Brodmann areas (BA) 24, 10, 32], posterior cingulate cortex/precuneus (BA 29, 30, 23, 31, 7), inferior parietal lobule/angular gyrus (BA 39, 40), lateral temporal cortex (BA 21), dorsal medial prefrontal cortex (BA 24, 32, 9, 10) and the hippocampal formation [for detailed reference see Table 1 in Buckner et al. (2008)]. Within this predefined network, we applied a significance threshold of $P < 0.001$ (uncorrected) across all imaging modalities, to allow comparability of the results, as previously published (Sperling et al., 2009). An extent threshold of 30 contiguous voxels was selected.

According to our hypothesis, we expected abnormalities, particularly in the posterior cingulate cortex/precuneus region. Thus, we employed an independently predefined spherical volume in the posterior cingulate cortex for volumes of interest-based group comparison (Andrews-Hanna et al., 2007). For this analysis a significance threshold of $P < 0.05$ was used.

Cross modality/correlation analyses

To quantitatively evaluate the topographical overlap between the patterns of whole-brain connectivity disruption and hypometabolism in mild cognitive impairment, we calculated a dice coefficient of similarity between the two findings (Zou et al., 2004).

Pearson correlation coefficients were calculated between values measured within the predefined volumes of interest (posterior cingulate cortex, FLR-VOI). Correlations were regarded significant above a threshold of $P < 0.05$. Additionally, correlation analyses between imaging and non-imaging findings were performed and voxel-based correlation analyses between imaging modalities were employed for regionally unrestricted correlation analysis (see Supplementary Material). For further detailed description of statistical methods refer to the Supplementary Material.

Results

Subject characteristics

On the basis of the preconditions mentioned above, we were able to collect data from 37 older subjects (mean age 74.0 ± 6.3) (Table 1), which included 24 cognitively normal healthy controls classified as PiB-positive (n = 12) or PiB-negative (n = 12). Thirteen of the subjects were PiB-positive with mild cognitive impairment

Table 1 Subject characteristics

Characteristics	PiB-negative healthy controls	PiB-positive healthy controls	PiB-positive patients with mild cognitive impairment
n (female/male)	12 (7/5)	12 (8/4)	13 (4/9)
PiB-FLR (mean ± SD)	1.07 ± 0.05	1.35 ± 0.20*	1.58 ± 0.34$^{\#,*}$
Age (mean ± SD)	71.3 ± 6.3	74.5 ± 5.7	75.9 ± 6.4
Clinical Dementia Rating Scale—global	0	0	0.5
Clinical Dementia Rating Scale—sum of boxes (mean ± SD)	0	0	1.83 ± 1.17$^{\#,*}$
MMSE (mean ± SD)	28.92 ± 0.79	29.42 ± 0.79	27.5 ± 2.43$^{\#}$
Years of education (mean ± SD)	17.36 ± 1.69	15.75 ± 3.17	17.75 ± 2.70

*Significant as compared to PiB-negative controls ($P < 0.05$); $^{\#}$Significant as compared to PiB-positive controls ($P < 0.05$).
MMSE = Mini Mental State Examination.

($n = 13$). The three groups were significantly different with regard to the PiB-FLR values, with the highest mean tracer uptake in subjects with mild cognitive impairment, followed by PiB-positive healthy controls and PiB-negative healthy controls (Table 2). The mean time span between the first and last imaging modality was 4.9 ± 1.8 months, and did not differ between the groups. There were no significant differences between the groups with regard to level of education and age. Nevertheless, age was included as covariate into the statistical analyses, as amyloid deposition is thought to be related to advancing age, and because the mean age was numerically highest in mild cognitive impairment, followed by PiB-positive healthy controls and PiB-negative healthy controls.

Voxel-based group comparisons

The whole-brain connectivity in the group of PiB-negative healthy controls revealed areas with a high degree of whole-brain connectivity (cortical hubs) distributed in a similar pattern as described in a previous study in healthy younger adults (Buckner *et al.*, 2009), with maxima in medial prefrontal cortex, bilateral parietal/angular cortex, posterior cingulate cortex/precuneus and bilateral lateral temporal cortex (Fig. 1A and Supplementary Table 1). In contrast, the PiB-positive healthy control group demonstrated no significant whole-brain connectivity clusters in right angular and posterior cingulate cortex/precuneus cortical hub regions and whole-brain connectivity clusters were completely absent in bilateral angular and posterior cingulate cortex/precuneus regions in the mild cognitive impairment group. Correspondingly, statistical comparison between the groups revealed a reduced degree of whole-brain connectivity in mild cognitive impairment as compared to PiB-negative healthy controls in posterior cortical hub regions, including angular, lateral temporal and the posterior cingulate cortex/precuneus regions (Fig. 1B and Supplementary Table 2). Whole-brain connectivity disruptions in left lateral temporal cortical regions were also detected in mild cognitive impairment as compared to PiB-positive healthy controls (Supplementary Fig. 1B and Supplementary Table 2). PiB-positive healthy controls revealed decreased whole-brain connectivity compared with PiB-negative healthy controls in right-hemispheric lateral temporal cortex, extending into the posterior cingulate cortex (Supplementary Fig. 1B and Supplementary Table 2).

In the ^{18}F-fluorodeoxyglucose-PET studies, statistical voxel-based group comparison between subjects with mild cognitive impairment and PiB-negative healthy controls revealed significant hypometabolism in subjects with mild cognitive impairment in dorsal brain regions, including posterior cingulate cortex/precuneus and extending into lateral temporal cortical areas (Fig. 1B and Supplementary Table 2). The topography of these abnormalities in subjects with mild cognitive impairment showed distinct anatomical overlap with the whole-brain connectivity abnormalities detected in the same group (Figs 1B and 2; Supplementary Table 2). Comparing subjects with mild cognitive impairment to PiB-positive healthy controls, hypometabolic changes were observed in subjects with mild cognitive impairment in the precuneus, resembling the pattern detected in comparison with PiB-negative healthy controls (Supplementary Fig. 1A and Supplementary Table 2). Comparison between PiB-positive healthy controls and PiB-negative healthy controls revealed only a small cluster of lower metabolism in right frontal cortex in PiB-positive healthy controls [Talairach coordinates (x, y, z): 56, 16, 26, z-score 3.99], which was outside of our network of expected

Table 2 Group comparison of values as measured in different imaging modalities by volume of interest-based analysis and volume of interest-based correlation analysis of values as measured in different imaging modalities in the entire sample

Groups/comparisons	PiB	FDG	WBC	VBM
Volume of interest-based group comparison*				
Groups				
HC-PiB$^-$	1.07 ± 0.05	65.67 ± 3.92	0.37 ± 0.69	86.15 ± 2.94
HC-PiB$^+$	1.35 ± 0.2	62.13 ± 3.34	0.06 ± 0.52	86.39 ± 5.10
MCI	1.58 ± 0.34	60.07 ± 3.80	-0.19 ± 0.37	85.23 ± 4.66
t-tests (*P*-values)				
HC-PiB$^-$ versus MCI	<0.001	0.001	0.021	0.897
HC-PiB$^+$ versus MCI	0.05	0.164	0.183	0.577
HC-PiB$^-$ versus HC-PiB$^+$	<0.001	0.027	0.241	0.581

Correlation analyses	No correction		Age corrected		Atrophy corrected	
	FDG	WBC	FDG	WBC	FDG	WBC
Volumes of interest-based correlation analysis#						
PiB	−0.56	−0.36	−0.57	−0.29	−0.53	−0.36
FDG	–	0.33	–	0.33	–	0.35

*Values are given as mean ± standard deviation.
#Values represent the Pearson correlation-coefficient, significance threshold: $P < 0.05$ (two-tailed).
FDG = ^{18}F-fluorodeoxyglucose-PET values in the spherical volume of interest in posterior cingulate cortex (posterior cingulate cortex-volume of interest); PiB = ^{11}C-PiB-PET values measured in the large cortical FLR-VOI; VBM = voxel-based morphometry values in the posterior cingulate cortex volume of interest, derived from structural MRI; WBC = whole-brain connectivity values in the posterior cingulate cortex volume of interest, derived from resting functional MRI. HC-PiB$^-$ = PiB-negative healthy controls; HC-PiB$^+$ = PiB-positive healthy controls; MCI = PiB-positive patients with mild cognitive impairment.

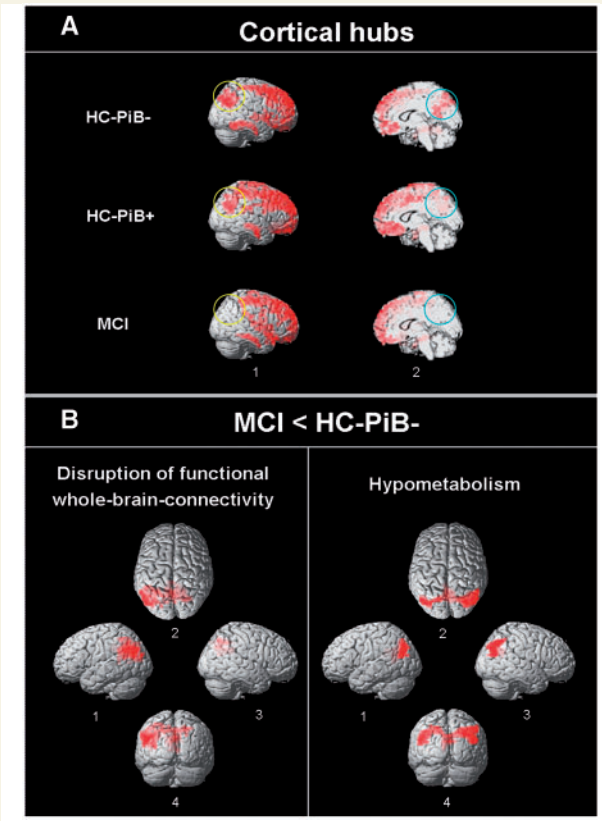

Figure 1 (**A**) Cortical hubs, identified by whole-brain functional connectivity analysis of resting state functional MRI in PiB-negative healthy controls (HC-PiB$^-$), PiB-positive healthy controls (HC-PiB$^+$) and PiB-positive patients with mild cognitive impairment (MCI). Regions affected by loss of cortical hubs in patients with mild cognitive impairment and PiB-positive healthy controls are labelled with circles on (1) lateral (yellow) and (2) medial (blue) aspects of the right hemisphere (contralateral results are comparable). (**B**) Voxel-based statistical group comparison between mild cognitive impairment and PiB-negative healthy controls. (*Left*) Hypometabolism in mild cognitive impairment as compared to PiB-negative healthy controls (^{18}F-fluorodeoxyglucose-PET). (*Right*) Disrupted cortical hubs in mild cognitive impairment as compared to PiB-negative healthy controls. Aspects: 1 = left lateral; 2 = cranial; 3 = right lateral; 4 = dorsal. Significance threshold $P < 0.001$ (uncorrected).

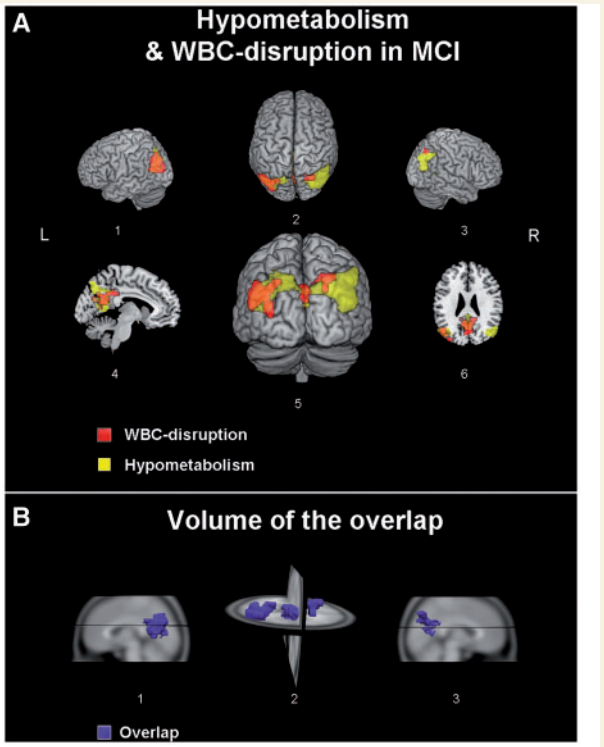

Figure 2 (**A**) 3D surface projection of the overlap between hypometabolic deficits (yellow) and regional disruption of whole-brain connectivity (WBC) (red) in PiB-positive patients with mild cognitive impairment (MCI) as compared to PiB-negative healthy controls at a threshold of $P < 0.001$ (uncorrected). Aspects: 1 = left lateral; 2 = cranial; 3 = right lateral; 4 = sagittal left medial; 5 = dorsal; 6 = axial caudal. (**B**) 3D volumetric illustration of the overlap between the abnormalities (in blue). Aspects: 1 = sagittal left lateral; 2 = dorsal; 3 = sagittal right lateral.

abnormalities. A cluster in the posterior cingulate cortex was just below the significance threshold (Talairach coordinates −4, −67, 14, *z*-score 2.97).

Voxel-based morphometry revealed only subtle focal reductions of grey matter density in subjects with mild cognitive impairment as compared with PiB-negative healthy controls in the right parahippocampal region (Supplementary Fig. 1C and Supplementary Table 2). Outside of the predefined network, clusters of reduced cortical density were detected in bilateral middle temporal and inferior frontal cortex as well as in left precentral cortex and in proximity to the ventricular system, e.g. adjacent to bilateral thalamic regions and the right caudate. However, none of these clusters showed overlap with the abnormalities observed in fluorodeoxyglucose-PET and whole-brain connectivity analysis in the different groups. Also compared with PiB-positive healthy controls, grey matter reductions were found in subjects with mild cognitive impairment in bilateral hippocampal/parahippocampal regions. Outside the expected network, clusters with reduced cortical density were observed in inferior temporal cortex as well as in left thalamic and middle occipital areas. Direct comparison between PiB-positive healthy controls and PiB-negative healthy controls only revealed minor reductions in the right precentral and middle frontal gyrus in PiB-positive healthy controls. None of the detected grey matter reductions showed major overlap with the changes observed in fluorodeoxyglucose-PET and whole-brain connectivity analysis in the different groups.

Anatomic overlap: dice coefficient of similarity

The fluorodeoxyglucose and whole-brain connectivity abnormalities detected in subjects with mild cognitive impairment by

voxel-based analysis showed striking regional overlap in posterior cingulate cortex/precuneus regions (Fig. 2). Quantitative analysis using the dice coefficient revealed that fluorodeoxyglucose and whole-brain connectivity abnormalities showed 42% similarity.

Volumes of interest-based group comparison

We employed an independently predefined spherical volume in the posterior cingulate cortex, which has been previously established (refer to the 'Materials and Methods' section and Supplementary Material) (Andrews-Hanna *et al*., 2007). Within the posterior cingulate cortex volume of interest, statistically significant reductions of cerebral metabolism were observed in patients with mild cognitive impairment but also in PiB-positive healthy controls, as compared to PiB-negative healthy controls (Fig. 3B and Table 2). Furthermore, a significantly reduced degree of whole-brain connectivity was observed within this volume of interest in patients with mild cognitive impairment, as compared with PiB-negative healthy controls. In PiB-positive healthy controls, whole-brain connectivity values were numerically lower as compared with PiB-negative healthy controls and higher as compared with subjects with mild cognitive impairment; however, due to high standard deviation, these differences did not reach significance (Fig. 3C and Table 2). No significant differences in grey matter density between subjects with mild cognitive impairment, PiB-negative healthy controls and PiB-positive healthy controls were found in volume of interest-based analysis.

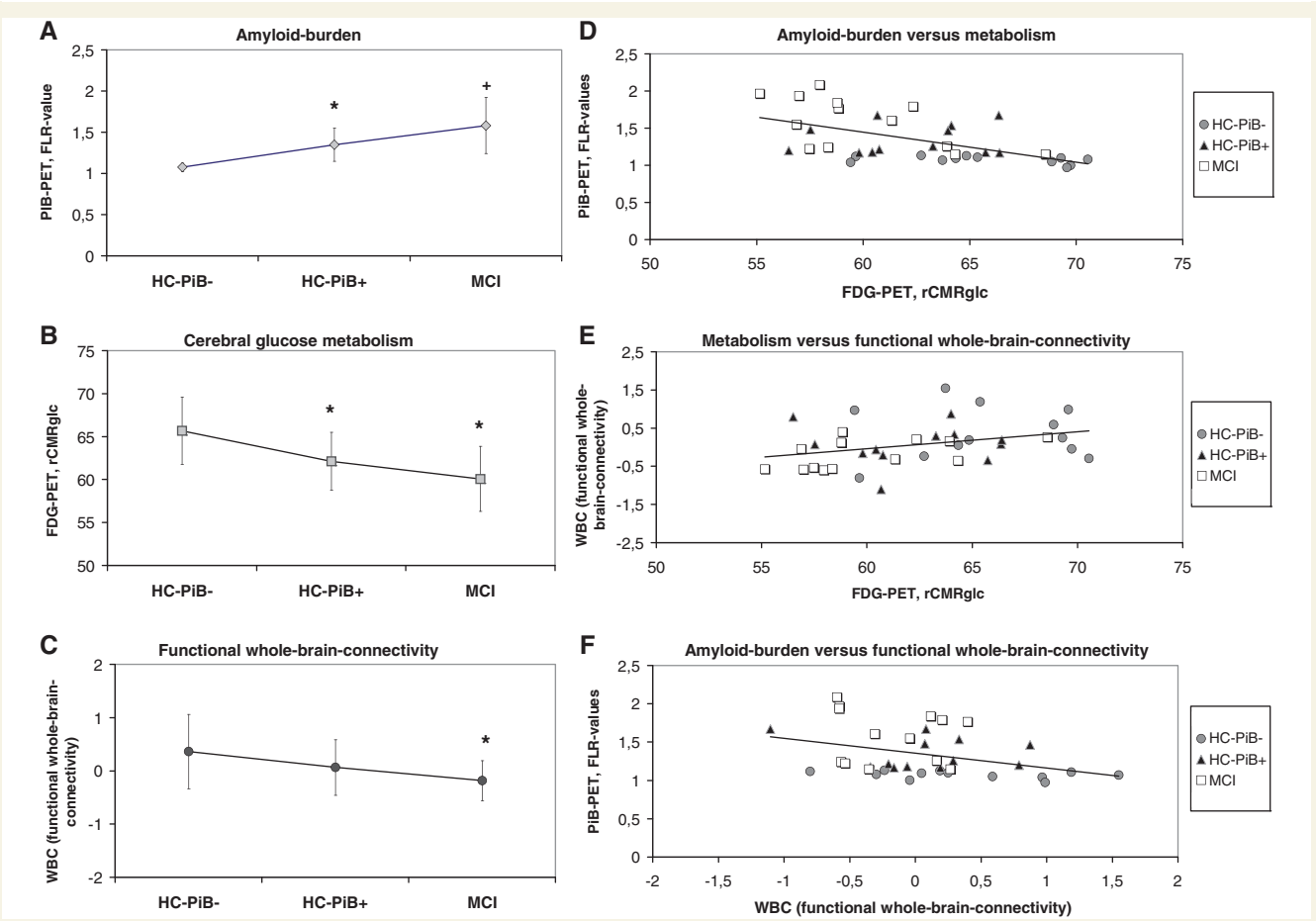

Figure 3 Volume of interest based group comparisons (*left*) and correlation analyses (*right*). *Left*: Mean and standard deviation of (**A**) glucose metabolism as measured by ^{18}F-fluorodeoxyglucose-PET, (**B**) amyloid burden measured by ^{11}C-PiB-PET and (**C**) whole-brain connectivity (WBC) (cortical hub integrity) as measured by resting-state functional MRI within the posterior cingulate cortex-volume of interest in PiB-negative healthy controls (HC PiB$^-$), PiB-positive healthy controls (HC PiB$^+$) and PiB-positive patients with mild cognitive impairment (MCI). Error bars refer to the standard deviations. *Right*: Correlation analyses between: (**D**) glucose metabolism (posterior cingulate cortex-volume of interest) and amyloid burden (FLR-VOI); (**E**) whole-brain connectivity (posterior cingulate cortex-volume of interest) and amyloid burden (FLR-VOI) and (**F**) glucose metabolism and whole-brain connectivity (both posterior cingulate cortex-volume of interest) as measured in the entire sample (including PiB-negative healthy controls, PiB-positive healthy controls and PiB-positive patients with mild cognitive impairment). Number of data points: $n = 37$. FDG-PET = fluorodeoxyglucose PET; PCC-VOI = independently predefined spherical volume of interest in the posterior cingulate cortex; rCMRglc = regional cerebral metabolic rate of glucose consumption; *Significant as compared with PiB-negative healthy controls (unpaired *t*-test, significance threshold $P < 0.05$). $^+$significant as compared with PiB-negative healthy controls and to PiB-positive healthy controls (unpaired *t*-test, significance threshold $P < 0.05$).

This indicates that differences in fluorodeoxyglucose and whole-brain connectivity were unlikely to be due to structural grey matter differences (Table 2).

Correlation analyses

In volume of interest-based correlation analysis of the imaging findings across our entire sample, significant negative correlations were found between PiB-FLR values and fluorodeoxyglucose-values in the posterior cingulate cortex as well as between PiB-FLR values and whole-brain connectivity values in the posterior cingulate cortex. A positive correlation was observed between fluorodeoxyglucose-values in the posterior cingulate cortex and whole-brain connectivity values in the posterior cingulate cortex values (Fig. 3D–F and Table 2). We also found a significant negative correlation between PiB-FLR values and fluorodeoxyglucose values in the posterior cingulate cortex ($r = -0.60$) and a trend towards a positive correlation between PiB-FLR and whole-brain connectivity values in the posterior cingulate cortex ($r = 0.54$, $P = 0.06$) in the mild cognitive impairment group alone. Including age and regional grey matter density as potential confounding variables into the analyses did not substantially alter the detected correlations between imaging modalities (Table 2). For additional results of voxel-based correlation analysis, see the Supplementary material.

Discussion

The findings of our study suggest a clear association between functional disconnection of cortical hubs, reduced neuronal activity and amyloid burden in predementia stages of Alzheimer's disease. The first key finding of the current study is the significant disruption of functional whole-brain connectivity in cortical hub regions (posterior cingulate/precuneus and temporoparietal cortex) in amyloid-positive mild cognitive impairment. Furthermore, characteristic hypometabolic abnormalities were also evident in this mild cognitive impairment sample, demonstrating major topographical overlap with the connectivity disruptions. Minor reductions of cerebral glucose metabolism and of functional whole-brain connectivity were found in amyloid-positive healthy subjects in corresponding brain areas. Across the entire sample, higher amyloid burden correlated with lower whole-brain connectivity and metabolism, particularly in the posterior cingulate cortex/precuneus. Inversely, a positive correlation between metabolism and whole-brain connectivity was found in this region, supporting the hypothesis of early amyloid-related dysfunction in this key hub region.

Our findings are consistent with several previously published single modality imaging studies in ageing and early Alzheimer's disease. Significantly increased uptake of the amyloid-tracer ^{11}C-PiB has been consistently documented in patients with Alzheimer's disease with manifest dementia but also in 50–60% of patients with mild cognitive impairment and even in 20–50% of elderly healthy subjects (Drzezga, 2010). First studies indicate a predictive value of elevated PiB uptake in non-demented subjects with regard to later cognitive decline, suggesting that these findings represent early Alzheimer's disease pathology (Mintun *et al*., 2006; Pike *et al*., 2007; Morris *et al*., 2009; Okello *et al*., 2009). Similar to previous studies, we quantified overall amyloid burden in a large cortical region to avoid bias towards a specific cortical region (Hedden *et al*., 2009). We divided subjects into amyloid-positive and negative according to pre-established cut-off values and we only included amyloid-positive subjects with mild cognitive impairment to increase the probability that they represent predementia Alzheimer's disease (Hedden *et al*., 2009).

To probe cortical hub integrity, we performed an analysis of regional whole-brain connectivity on the resting functional MRI data. With the same technique as applied in our recent study, functional cortical hubs were consistently identified in a group of 127 young healthy controls, with maxima in bilateral parietal lobules, the posterior cingulate cortex, medial frontal and superior/middle frontal cortical regions (Buckner *et al*., 2009). We identified a similar pattern of intact cortical hubs in PiB-negative healthy controls in our study. In contrast, significant whole-brain connectivity disruption was detected in patients with mild cognitive impairment in temporoparietal cortex and posterior cingulate cortex/precuneus, i.e. typical cortical hub regions. In similar regions, significant whole-brain connectivity disruptions were even found in PiB-positive healthy controls, pointing to early functional abnormalities in this group, possibly long before onset of dementia. To our knowledge this is the first study demonstrating disruption of functional whole-brain connectivity in subjects at risk for Alzheimer's disease. As these cortical hubs are thought to play a critical role in mediating inter-regional communication in the brain (Buckner *et al*., 2009; Sepulcre *et al*., 2010), the breakdown of these important switch points may contribute to progressive cognitive dysfunction in Alzheimer's disease. In addition to these findings, we identified significant hypometabolism with ^{18}F-fluorodeoxyglucose-PET in subjects with mild cognitive impairment, particularly in the posterior cingulate cortex/precuneus. Since synaptic activity of neurons is associated with glucose uptake, cerebral hypometabolism can be regarded as a measure of reduced neuronal activity (Magistretti and Pellerin, 1999). The hypometabolic abnormalities detected in our study correspond well to findings reported in previous studies in patients with Alzheimer's disease and with progressive mild cognitive impairment, supporting the notion that our mild cognitive impairment population included subjects with early Alzheimer's disease pathology (Herholz, 1995; Silverman *et al*., 2001; Minoshima, 2003; Mosconi *et al*., 2004; Drzezga *et al*., 2005; Reiman *et al*., 2005; Nobili *et al*., 2008). The patterns of hypometabolism and regional cortical hub disruption in mild cognitive impairment showed striking similarity, with a topographical overlap of 42%, indicating that the two different functional abnormalities are distinctly regionally interrelated. Volume of interest-based analysis revealed significantly lower metabolism in the posterior cingulate cortex also in PiB-positive healthy controls, indicating minor metabolic abnormalities were already present in this cognitively intact group. Altogether, these findings suggest that emerging amyloid burden may initiate synaptic dysfunction and disruptions in the connectivity in corresponding regions.

These findings are further complemented by the cross-modality correlation analyses. The positive correlation between metabolism and cortical hub integrity (whole-brain connectivity values) observed in posterior cortical hub regions supports the notion

that neuronal dysfunction and functional disconnection in these areas may be causally interwoven. Interestingly, lower fluorodeoxyglucose-PET values in the posterior cingulate cortex region were correlated with lower whole-brain connectivity values not only in the posterior cingulate cortex/precuneus, but also in frontal and cortical regions in unrestricted voxel-based analysis (see Supplementary Material). Thus, synaptic dysfunction in the posterior cingulate cortical hub may affect function of remote brain regions and potentially foster the onset of neurodegeneration in these regions. This underlines the importance of intact neuronal function in the posterior cingulate cortex as a major cortical hub. The finding that higher overall amyloid burden was correlated with lower metabolism and whole-brain connectivity values in the posterior cingulate cortex/precuneus region suggests that cortical hub regions may be particularly vulnerable to subsequent neurodegeneration induced by elevated amyloid burden. The values used for the correlation analyses showed a continuous distribution with a relatively broad overlap between the three samples rather then group-centred clusters. This indicates that the detected correlations may not have been only driven by group-based differences. Supporting this impression, a strong negative correlation between amyloid burden and fluorodeoxyglucose-PET values was also present in the mild cognitive impairment sample alone. However, the detected correlations may still in part be based on the differences between the three groups.

To investigate whether both hypometabolic and functional connectivity changes observed in our study might be due to cortical brain atrophy as a common underlying pathology, we performed a voxel based morphometry analysis of the structural MRI data from all subjects. This analysis revealed focal reductions in cortical grey matter density in mild cognitive impairment in a pattern corresponding well to results from several previous studies (Bell-McGinty *et al*., 2005; Whitwell *et al*., 2007). The observed grey matter reductions did not show essential overlap with the abnormalities detected by fluorodeoxyglucose-PET or functional MRI. Only in PiB-positive healthy controls, a small reduction in middle frontal grey matter density may account for the subtle hypometabolism observed at the same location. In addition, the volume of interest-based analyses support the notion that the observed functional changes, as measured with fluorodeoxyglucose-PET and functional MRI, were not mainly the result of regional cortical atrophy. We did not perform partial volume correction of our PET data, as there is no generally accepted method available for partial volume correction of functional MRI resting state data, particularly not for the recently introduced cortical hub analyses and we preferred to compare all different imaging modalities on the same structural framework. Consequently, some effect of regional atrophy on our results cannot be excluded, although results from voxel-based morphometry analysis do not point in this direction.

Regarding the interrelation between amyloid burden, functional connectivity and metabolism, information from previous studies is very limited. Impaired functional connectivity in the default mode network has been demonstrated not only in Alzheimer's disease and mild cognitive impairment but also in PiB-positive healthy controls, particularly affecting connectivity to/from the posterior cingulate cortex/precuneus region (Rombouts *et al*., 2005; Sorg *et al*., 2007; Hedden *et al*., 2009). It can be speculated that a breakdown of cortical hub function may also have contributed to those results. In another recent study, Cohen *et al.* (2009) demonstrated inverse correlations between amyloid burden and cerebral metabolism in parietal and precuneus cortex in patients with manifest Alzheimer's disease, corresponding well to our findings. However, in contrast to our findings, they observed positive correlations between metabolism and PiB uptake in mild cognitive impairment in several regions, and they did not observe a correlation between PiB- and fluorodeoxyglucose-PET values in amyloid-positive controls. However, in contrast to our study, Cohen *et al*. (2009) related PiB to fluorodeoxyglucose data in a specific region-to-region comparison, whereas we assessed overall amyloid burden. Importantly, Cohen *et al.* (2009) applied partial volume correction to their PET data, whereas we did not (for the reasons explained above). This may also in part explain the differences between the studies. Finally, hypometabolic abnormalities have been described in mild cognitive impairment in many previous studies (Silverman *et al*., 2001; Chetelat *et al*., 2003; Minoshima, 2003; Mosconi *et al*., 2004; Drzezga *et al*., 2005), which may also indicate that patients with mild cognitive impairment examined by Cohen *et al*. (2009) may have been in earlier stages of disease than those included in other studies.

Mechanistically, the findings of our study can be interpreted in different ways: (i) subtle neuronal loss in cortical hub regions (undetected by voxel based morphometry analysis) may have led to reduced regional energy consumption (hypometabolism) and reduction of functional connectivity; (ii) synaptic dysfunction in the affected areas may have led to reduced connectivity to other brain regions resulting in lower energy consumption. Vice versa, reduced metabolic/energetic efficiency may have led to impaired energy provision, limiting synaptic communication with other brain regions; and (iii) reduced neuronal function of remote brain regions may have led to reduced input into the cortical hub regions, resulting in reduced synaptic activity and neuronal energy requirement. Currently, it remains unknown if the blood oxygen level-dependent signal in functional MRI studies is driven by regional neuronal output (spikes) or input from remote neurons (local field potentials) (Raichle and Mintun, 2006). Thus, a mixture of all three hypotheses may explain our results. It has been recently suggested that specific properties of cortical hubs may directly augment the pathological cascade of Alzheimer's disease. An anatomical connection with numerous other brain regions may lead to high functional tension in these regions, i.e. continuously high levels of activity may predispose them for later neurodegeneration (Buckner *et al*., 2009). It has been demonstrated that processing of amyloid peptides depends on regional synaptic activity (Nitsch *et al*., 1993; Cirrito *et al*., 2005) and that aggregated β-amyloid peptides may exert a direct synaptotoxic effect (Hardy and Higgins, 1992; Selkoe, 2008). These facts may predispose cortical hubs for excessive β-amyloid accumulation and consecutive neurodegeneration. In line with this theory, overlap between cortical hub locations in healthy controls and β-amyloid deposition in patients with Alzheimer's disease has been shown (Buckner *et al*., 2005, 2009). Complementing these findings, it has been observed that cortical hubs are among the brain regions that demonstrate high levels of 'aerobic glycolysis' (excessive glycolysis

despite the presence of oxygen) (Raichle, 2006; Vaishnavi *et al*., 2010). Recently, genetic variation in glyceraldehyde-3-phosphate dehydrogenase (GAPDH), a key enzyme of glycolysis, has been proposed as a risk factor for Alzheimer's disease, indicating a connection between glycolysis and neurodegeneration (Li *et al*., 2004). It has been speculated that regions dependent on aerobic glycolysis may be particularly susceptible to failure of vital mechanisms such as glucose-dependent synaptic function or protection from oxidative stress. Correspondingly, a spatial correlation between aerobic glycolysis and amyloid deposition has recently been demonstrated in Alzheimer's disease and PiB-positive healthy controls (Vlassenko *et al*., 2010), including regions affected by overlapping hypometabolism and whole-brain connectivity disruption in our study.

Several limitations apply to our study. We hypothesized that groups of mild cognitive impairment and PiB-positive healthy controls represent individuals in predementia stages of Alzheimer's disease. Although, many recent studies point in this direction, these assumptions can only be verified by long-term clinical follow-up studies. Furthermore, we compared findings derived from different imaging techniques, which may have different methodological sensitivity. The results of our study neither clarify causality of the relationships nor the chronological appearance of the biomarkers. We did not perform partial volume correction of the PET data in our study and voxel-based morphometry analysis may have missed some more subtle structural changes, e.g. in grey matter thickness. Thus, some effects of regional structural differences cannot be excluded. It has been demonstrated that the *ApoE* genotype may have a relevant impact on the presence and degree of cerebral abnormalities associated with Alzheimer's disease, thus, different *ApoE* genotypes may also have influenced the parameters examined here (see Supplementary Material). This problem could not be sufficiently addressed in the current study, as we did not have *ApoE* genotype available for all of our subjects. It may be an interesting subject for future studies to examine the effect of the *ApoE* genotype on the interaction of different brain pathologies associated with Alzheimer's disease. Finally, the clinical subgroups in our study were relatively small and group size and gender distribution were not perfectly matched. Thus, the findings from the current study should be replicated in future studies including larger samples.

In conclusion, we found anatomically overlapping disruptions of functional whole-brain connectivity and hypometabolism in amyloid-positive patients with mild cognitive impairment in posterior brain regions (posterior cingulate/precuneus). To a lesser extent, similar abnormalities were already present in corresponding regions in amyloid-positive older adults without cognitive symptoms. Both regional disruption of connectivity and hypometabolism were associated with increasing amyloid burden across all subjects, which indicates that they may represent early functional consequences of molecular Alzheimer's disease pathology, evolving prior to clinical onset of dementia. The interrelation between hypometabolism and disruption of functional connectivity may reflect a link between synaptic failure and functional disconnection. The concentration of these abnormalities in specific cortical hub areas indicates that these regions may be particularly susceptible to early Alzheimer's disease neurodegeneration, perhaps due to the increased metabolic demands of maintaining high connectivity. Dysfunction of cortical hubs may represent an important early pathophysiological feature of Alzheimer's disease, contributing to progressive cognitive impairment.

Acknowledgements

We thank Dr Randy Buckner for his valuable comments on this project, Mary Foley, Larry White and the Athinoula A. Martinos Center MRI Core for assistance with MR imaging, the Massachusetts General Hospital Molecular Imaging PET Core for providing assistance with PiB-PET imaging, Drs Bill Klunk and Chet Mathis from the University of Pittsburgh for advice on PiB imaging and analysis, the Massaschusetts Alzheimer's Disease Research Center (ADRC) and Dr Liang Yap for assistance with subject recruitment, Dr Dorene Rentz, Meghan Frey, Elisha Eng and Lauren Olson for assistance with neuropsychological testing, Drs Gregory Sorensen and Ciprian Catana for advice and support.

Funding

Funding for this study has been provided by: The German Research Foundation (Deutsche Forschungsgemeinschaft, DFG) (DR 445/3-1, 4-1 to A.D.), the National Institute on Aging (R01AG027435 to R.A.S. and K.A.J.), the Alzheimer's Disease Research Center (ADRC) (P50AG005134 to R.A.S. and K.A.J., P01 AG036694 to R.A.S.), an Anonymous Medical Foundation (to R.A.S. and K.A.J.) and the Alzheimer's Association (to R.A.S.).

Conflict of interest

Dr Keith Johnson has consulted for GE Healthcare, who holds the commercial licensing and distribution rights for PiB PET imaging.

Supplementary material

Supplementary Material is available at *Brain* online.

References

Andrews-Hanna JR, Snyder AZ, Vincent JL, Lustig C, Head D, Raichle ME, et al. Disruption of large-scale brain systems in advanced aging. Neuron 2007; 56: 924–35.

Ashburner J, Friston KJ. Unified segmentation. Neuroimage 2005; 26: 839–51.

Beckmann CF, DeLuca M, Devlin JT, Smith SM. Investigations into resting-state connectivity using independent component analysis. Philos Trans R Soc Lond B Biol Sci 2005; 360: 1001–13.

Bell-McGinty S, Lopez OL, Meltzer CC, Scanlon JM, Whyte EM, Dekosky ST, et al. Differential cortical atrophy in subgroups of mild cognitive impairment. Arch Neurol 2005; 62: 1393–7.

Biswal B, Yetkin FZ, Haughton VM, Hyde JS. Functional connectivity in the motor cortex of resting human brain using echo-planar MRI. Magn Reson Med 1995; 34: 537–41.

Braak E, Griffing K, Arai K, Bohl J, Bratzke H, Braak H. Neuropathology of Alzheimer's disease: what is new since A. Alzheimer? Eur Arch Psychiatry Clin Neurosci 1999; 249 (Suppl 3): 14–22.

Buckner RL, Andrews-Hanna JR, Schacter DL. The brain's default network: anatomy, function, and relevance to disease. Ann NY Acad Sci 2008; 1124: 1–38.

Buckner RL, Sepulcre J, Talukdar T, Krienen FM, Liu H, Hedden T, et al. Cortical hubs revealed by intrinsic functional connectivity: mapping, assessment of stability, and relation to Alzheimer's disease. J Neurosci 2009; 29: 1860–73.

Buckner RL, Snyder AZ, Shannon BJ, LaRossa G, Sachs R, Fotenos AF, et al. Molecular, structural, and functional characterization of Alzheimer's disease: evidence for a relationship between default activity, amyloid, and memory. J Neurosci 2005; 25: 7709–17.

Calhoun VD, Adali T, Pearlson GD, Pekar JJ. A method for making group inferences from functional MRI data using independent component analysis. Hum Brain Mapp 2001; 14: 140–51.

Chetelat G, Desgranges B, de la Sayette V, Viader F, Eustache F, Baron JC. Mild cognitive impairment: Can FDG-PET predict who is to rapidly convert to Alzheimer's disease? Neurology 2003; 60: 1374–7.

Cirrito JR, Yamada KA, Finn MB, Sloviter RS, Bales KR, May PC, et al. Synaptic activity regulates interstitial fluid amyloid-beta levels in vivo. Neuron 2005; 48: 913–22.

Cohen AD, Price JC, Weissfeld LA, James J, Rosario BL, Bi W, et al. Basal cerebral metabolism may modulate the cognitive effects of Abeta in mild cognitive impairment: an example of brain reserve. J Neurosci 2009; 29: 14770–8.

Dickerson BC, Salat DH, Greve DN, Chua EF, Rand-Giovannetti E, Rentz DM, et al. Increased hippocampal activation in mild cognitive impairment compared to normal aging and AD. Neurology 2005; 65: 404–11.

Drzezga A. Concept of functional imaging of memory decline in Alzheimer's disease. Methods 2008; 44: 304–14.

Drzezga A. Amyloid-plaque imaging in early and differential diagnosis of dementia. Ann Nucl Med 2010; 24: 55–66.

Drzezga A, Grimmer T, Henriksen G, Muhlau M, Perneczky R, Miederer I, et al. Effect of APOE genotype on amyloid plaque load and gray matter volume in Alzheimer disease. Neurology 2009; 72: 1487–94.

Drzezga A, Grimmer T, Henriksen G, Stangier I, Perneczky R, Diehl-Schmid J, et al. Imaging of amyloid plaques and cerebral glucose metabolism in semantic dementia and Alzheimer's disease. Neuroimage 2008; 39: 619–33.

Drzezga A, Grimmer T, Riemenschneider M, Lautenschlager N, Siebner H, Alexopoulus P, et al. Prediction of individual clinical outcome in MCI by means of genetic assessment and (18)F-FDG PET. J Nucl Med 2005; 46: 1625–32.

Fleisher AS, Sherzai A, Taylor C, Langbaum JB, Chen K, Buxton RB. Resting-state BOLD networks versus task-associated functional MRI for distinguishing Alzheimer's disease risk groups. Neuroimage 2009; 47: 1678–90.

Friston KJ, Holmes AP, Worsley KJ, Poline J-B, Frith CD, Frackowiak RSJ. Statistical parametric mapping in functional imaging: a general linear approach. Hum Brain Mapp 1995; 2: 189–210.

Gomperts SN, Rentz DM, Moran E, Becker JA, Locascio JJ, Klunk WE, et al. Imaging amyloid deposition in Lewy body diseases. Neurology 2008; 71: 903–10.

Greicius MD, Srivastava G, Reiss AL, Menon V. Default-mode network activity distinguishes Alzheimer's disease from healthy aging: evidence from functional MRI. Proc Natl Acad Sci USA 2004; 101: 4637–42.

Gusnard DA, Raichle ME. Searching for a baseline: functional imaging and the resting human brain. Nat Rev Neurosci 2001; 2: 685–94.

Hardy JA, Higgins GA. Alzheimer's disease: the amyloid cascade hypothesis. Science 1992; 256: 184–5.

Hedden T, Van Dijk KR, Becker JA, Mehta A, Sperling RA, Johnson KA, et al. Disruption of functional connectivity in clinically normal older adults harboring amyloid burden. J Neurosci 2009; 29: 12686–94.

Herholz K. FDG PET and differential diagnosis of dementia. Alzheimer Dis Assoc Disord 1995; 9: 6–16.

Jack CR Jr, Lowe VJ, Senjem ML, Weigand SD, Kemp BJ, Shiung MM, et al. 11 C PiB and structural MRI provide complementary information in imaging of Alzheimer's disease and amnestic mild cognitive impairment. Brain 2008; 131: 665–80.

Johnson KA, Gregas M, Becker JA, Kinnecom C, Salat DH, Moran EK, et al. Imaging of amyloid burden and distribution in cerebral amyloid angiopathy. Ann Neurol 2007; 62: 229–34.

Kantarci K, Jack CR Jr. Quantitative magnetic resonance techniques as surrogate markers of Alzheimer's disease. NeuroRx 2004; 1: 196–205.

Li Y, Nowotny P, Holmans P, Smemo S, Kauwe JS, Hinrichs AL, et al. Association of late-onset Alzheimer's disease with genetic variation in multiple members of the GAPD gene family. Proc Natl Acad Sci USA 2004; 101: 15688–93.

Magistretti PJ, Pellerin L. Cellular mechanisms of brain energy metabolism and their relevance to functional brain imaging. Philos Trans R Soc Lond B Biol Sci 1999; 354: 1155–63.

Mathis CA, Bacskai BJ, Kajdasz ST, McLellan ME, Frosch MP, Hyman BT, et al. A lipophilic thioflavin-T derivative for positron emission tomography (PET) imaging of amyloid in brain. Bioorg Med Chem Lett 2002; 12: 295–8.

Minoshima S. Imaging Alzheimer's disease: clinical applications. Neuroimaging Clin N Am 2003; 13: 769–80.

Mintun MA, Larossa GN, Sheline YI, Dence CS, Lee SY, Mach RH, et al. [11C]PIB in a nondemented population: potential antecedent marker of Alzheimer disease. Neurology 2006; 67: 446–52.

Morris JC, Roe CM, Grant EA, Head D, Storandt M, Goate AM, et al. Pittsburgh compound B imaging and prediction of progression from cognitive normality to symptomatic Alzheimer disease. Arch Neurol 2009; 66: 1469–75.

Mosconi L, Perani D, Sorbi S, Herholz K, Nacmias B, Holthoff V, et al. MCI conversion to dementia and the APOE genotype: a prediction study with FDG-PET. Neurology 2004; 63: 2332–40.

Nitsch RM, Farber SA, Growdon JH, Wurtman RJ. Release of amyloid beta-protein precursor derivatives by electrical depolarization of rat hippocampal slices. Proc Natl Acad Sci USA 1993; 90: 5191–3.

Nobili F, Salmaso D, Morbelli S, Girtler N, Piccardo A, Brugnolo A, et al. Principal component analysis of FDG PET in amnestic MCI. Eur J Nucl Med Mol Imaging 2008; 35: 2191–202.

Okello A, Koivunen J, Edison P, Archer HA, Turkheimer FE, Nagren K, et al. Conversion of amyloid positive and negative MCI to AD over 3 years. An 11 C-PIB PET study. Neurology 2009; 73: 754–60.

Pike KE, Savage G, Villemagne VL, Ng S, Moss SA, Maruff P, et al. Beta-amyloid imaging and memory in non-demented individuals: evidence for preclinical Alzheimer's disease. Brain 2007; 130: 2837–44.

Price JC, Klunk WE, Lopresti BJ, Lu X, Hoge JA, Ziolko SK, et al. Kinetic modeling of amyloid binding in humans using PET imaging and Pittsburgh Compound-B. J Cereb Blood Flow Metab 2005; 25: 1528–47.

Raichle ME. Neuroscience. The brain's dark energy. Science 2006; 314: 1249–50.

Raichle ME, MacLeod AM, Snyder AZ, Powers WJ, Gusnard DA, Shulman GL. A default mode of brain function. Proc Natl Acad Sci USA 2001; 98: 676–82.

Raichle ME, Mintun MA. Brain work and brain imaging. Annu Rev Neurosci 2006; 29: 449–76.

Reiman EM, Chen K, Alexander GE, Caselli RJ, Bandy D, Osborne D, et al. Correlations between apolipoprotein E epsilon4 gene dose and brain-imaging measurements of regional hypometabolism. Proc Natl Acad Sci USA 2005; 102: 8299–302.

Rombouts SA, Barkhof F, Goekoop R, Stam CJ, Scheltens P. Altered resting state networks in mild cognitive impairment and mild Alzheimer's disease: an fMRI study. Hum Brain Mapp 2005; 26: 231–9.

Selkoe DJ. Soluble oligomers of the amyloid beta-protein impair synaptic plasticity and behavior. Behav Brain Res 2008; 192: 106–13.

Sepulcre J, Liu H, Talukdar T, Martincorena I, Yeo BT, Buckner RL. The organization of local and distant functional connectivity in the human brain. PLoS Comput Biol 2010; 6: e1000808.

Sheline YI, Price JL, Yan Z, Mintun MA. Resting-state functional MRI in depression unmasks increased connectivity between networks via the dorsal nexus. Proc Natl Acad Sci USA 2010; 107: 11020–5.

Silverman DH, Small GW, Chang CY, Lu CS, Kung De Aburto MA, Chen W, et al. Positron emission tomography in evaluation of dementia: Regional brain metabolism and long-term outcome. Jama 2001; 286: 2120–7.

Sorg C, Riedl V, Muhlau M, Calhoun VD, Eichele T, Laer L, et al. Selective changes of resting-state networks in individuals at risk for Alzheimer's disease. Proc Natl Acad Sci USA 2007; 104: 18760–5.

Sperling RA, Laviolette PS, O'Keefe K, O'Brien J, Rentz DM, Pihlajamaki M, et al. Amyloid deposition is associated with impaired default network function in older persons without dementia. Neuron 2009; 63: 178–88.

Tomasi D, Volkow ND. Functional connectivity density mapping. Proc Natl Acad Sci USA 2010; 107: 9885–90.

Vaishnavi SN, Vlassenko AG, Rundle MM, Snyder AZ, Mintun MA, Raichle ME. Regional aerobic glycolysis in the human brain. Proc Natl Acad Sci USA 2010; 107: 17757–62.

Vincent JL, Snyder AZ, Fox MD, Shannon BJ, Andrews JR, Raichle ME, et al. Coherent spontaneous activity identifies a hippocampal-parietal memory network. J Neurophysiol 2006; 96: 3517–31.

Vlassenko AG, Vaishnavi SN, Couture L, Sacco D, Shannon BJ, Mach RH, et al. Spatial correlation between brain aerobic glycolysis and amyloid-{beta} (A{beta}) deposition. Proc Natl Acad Sci USA 2010; 107: 17763–7.

Whitwell JL, Przybelski SA, Weigand SD, Knopman DS, Boeve BF, Petersen RC, et al. 3D maps from multiple MRI illustrate changing atrophy patterns as subjects progress from mild cognitive impairment to Alzheimer's disease. Brain 2007; 130: 1777–86.

Yakushev I, Landvogt C, Buchholz HG, Fellgiebel A, Hammers A, Scheurich A, et al. Choice of reference area in studies of Alzheimer's disease using positron emission tomography with fluorodeoxyglucose-F18. Psychiatry Res 2008; 164: 143–53.

Ziolko SK, Weissfeld LA, Klunk WE, Mathis CA, Hoge JA, Lopresti BJ, et al. Evaluation of voxel-based methods for the statistical analysis of PIB PET amyloid imaging studies in Alzheimer's disease. Neuroimage 2006; 33: 94–102.

Zou KH, Warfield SK, Bharatha A, Tempany CM, Kaus MR, Haker SJ, et al. Statistical validation of image segmentation quality based on a spatial overlap index. Acad Radiol 2004; 11: 178–89.